

INTERFEROMETRIC SYNTHETIC APERTURE RADAR FOR TERRAIN MAPPING

John C. Curlander
Vexcel Corporation
2477 55th Street
Boulder, CO 80301 USA
Tel: 303/444-0094
Fax: 303/444-0470
E-mail: jcc@vexcel.com

ABSTRACT

This paper describes a new technique for topographic mapping using an interferometric synthetic aperture radar (IFSAR). The IFSAR utilizes microwave interference for precise measurement of small linear displacements related to the surface topography. It is similar to a traditional SAR system except that it has two receive antennas (with essentially the same boresight) and the single recording channel is replaced by two independent channels one for each antenna. From each imaging pass, the IFSAR measures (in addition to the backscattered power) the relative range distance from each antenna to the target pixel. The direct measurement is a relative phase difference which is related to the range diversity between the two antennas and the target area by the wavenumber. Using the relative phase difference in conjunction with the ranging and Doppler information, we can solve directly for the 3-D target location to produce a 3-D map of the target area without any earth model assumption.

1. INTRODUCTION

A conventional synthetic aperture radar (SAR), uses backscattered microwave energy to create a map of reflectivity measurements in two dimensions (range and cross range) as shown in Fig. 1.

To present these data as a two dimensional radar image map, some assumption is needed about the third dimension, the surface topography. The typical assumption is to create an oblate ellipsoid earth surface model onto which radar image pixels are projected as shown in Fig. 2. A detailed description of the technique to locate a SAR image pixel in three dimensional (3-D) space given an earth model was given by Curlander (1982).

In this paper we replace the surface model assumption in the pixel location solution by adding surface scattering measurements collected by a second radar antenna in an interferometric SAR (IFSAR) mode. An interferometric SAR is similar to a traditional SAR system except that it has two receive antennas (with essentially the same boresight) and independent data recording channels as shown in Figure 3 (Zebker and Goldstein, 1986). It utilizes the wave interference phenomenon (similar to

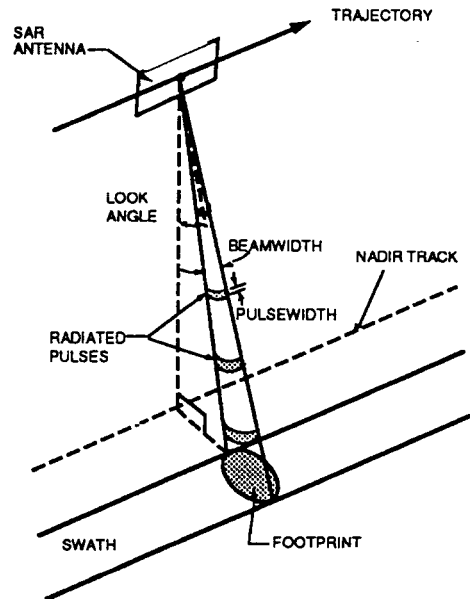


Figure 1. Conventional SAR imaging geometry.

light interferometry) for precise measurement of small linear displacements (i.e., the surface topography).

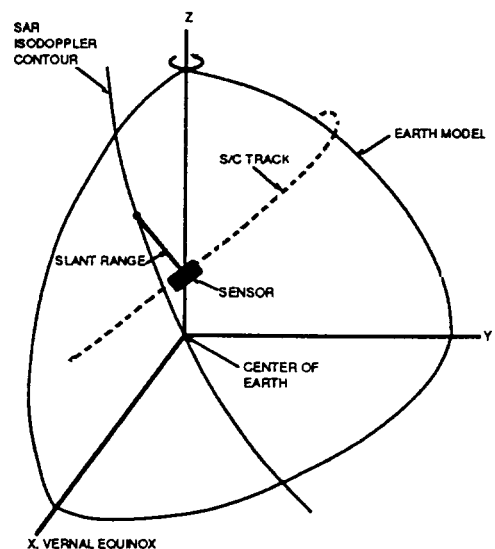


Figure 2. Geometric solution to SAR pixel location for oblate ellipsoid earth model.

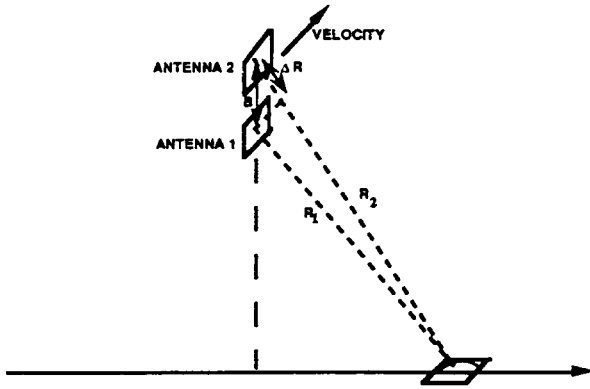


Figure 3. Imaging configuration of IFSAR system.

In an imaging pass, the IFSAR measures (in addition to the backscattered power) the relative range distance from each antenna to the target pixel. The direct measurement is a relative phase difference which is related to the range difference between the two antennas and the target area by the wavenumber $2\pi/\lambda$. Using this relative phase difference in conjunction with the ranging and Doppler information, we can solve directly for the 3-D target location to produce a 3-D map of the target area without any earth model assumption.

To understand generally how an interferometer measures relative phase, consider the following basic property of signals. Two waves, each of intensity I_0 , propagating in the z direction displaced by a distance d , can be represented by

$$s_1 = \sqrt{I_0} e^{-jkz}$$

and

$$s_2 = \sqrt{I_0} e^{-jk(z-d)}$$

The superposition of these two waves is a resultant wave whose phase is dependent on their relative displacement as given by

$$I = 2 I_0 [1 + \cos(2\pi d/\lambda)]$$

An interferogram is a record of relative phase change as measured by two receiving systems separated in space. Thus for an IFSAR if the antennas are oriented along an axis orthogonal to the line of flight at different ranges to the target, the superposition of the electromagnetic (EM) waves received by each antenna will produce a resultant EM wave whose phase is dependent on the displacement of these two waves. This interferogram can be converted into a map reflecting the relative height variation within the target area. The following section presents a theoretical solution to deriving the 3-D target location that is robust for mapping large areas.

2. THEORETICAL SOLUTION

When an interferometric SAR is employed, each backscatter measurement can be associated with a three geometric measurements (slant range, Doppler frequency and interferometric phase difference). These three measurements can through a closed form solution be used to derive the three-dimensional location of an image pixel (x, y, z) . From this absolute location, using a standard datum for the earth surface a terrain digital elevation model (DEM) can be produced.

The solution for the $\{x, y, z\}$ coordinate of a pixel in the IFSAR image requires three equations describing that pixel in terms of its $\{x, y, z\}$ coordinates. These three equations are:

- Range sphere equation
- Doppler cone equation
- Interferometric phase difference cone equation

The $\{x, y, z\}$ coordinate of a pixel are found by solving the above 3 equations for the unknown $\{x, y, z\}$ location of the target. The remainder of this section will more exactly define these equations.

2.1 Range Sphere Equation

A radar is a ranging instrument that essentially measures the time delay from the transmission of an echo to its reception. This delay is related to the slant range by the speed of light, c , as follows:

$$R = \frac{c}{2} = |\vec{R}_t - \vec{R}_s|$$

where

\vec{R}_t - target position vector (the unknown quantity)

\vec{R}_s - platform position vector (from platform state)

R - measured slant range (based on pulse echo time)

The target \vec{R}_t lies on a sphere of radius R centered at the instantaneous platform position \vec{R}_s .

2.2 Doppler Cone Equation

A radar can also measure the Doppler shift of the return echo data by a spectral analysis of the video echo signal. The Doppler centroid of the resulting azimuth spectrum, f_D is given by:

$$f_D = \frac{W_D}{2\pi} = \frac{2}{\lambda} \hat{p} \cdot (\vec{V}_s - \vec{V}_t)$$

where:

λ - radar wavelength

\hat{p} - pointing vector, platform to target

\vec{V}_s - velocity of platform

$\vec{V}_t = \frac{d}{dt} \vec{R}_t$ - velocity of target $\equiv 0$ in fixed earth coordinate system

The Doppler equation describes a cone with apex at the sensor antenna phase center with its axis along the relative (sensor to target) velocity vector. The apex angle is given by:

$$\cos \alpha = \frac{\lambda}{|\vec{V}_s|} \frac{f_D}{2}$$

For the Doppler equation, the correct value of the Doppler centroid to use for pixel location is not the true centroid, but the Doppler centroid actually used in the spectral analysis or matched filtering processing of the raw signal data.

2.3 Interferometric Phase Difference Cone Equation

The interferometric SAR phase difference is obtained by processing the two received signals to complex imagery and multiplying one image times the complex conjugate of the other. The argument of the resulting complex image is the 'wrapped IFSAR phase difference. This phase must first be unwrapped (Goldstein, et al, 1988) and the resulting absolute phase difference can be related to the target position as follows:

$$2\vec{B} \cdot (\vec{R}_t - \vec{R}_s) + (\delta R^2 + 2R\delta R - \vec{B}^2) = 0$$

where:

$$\delta R = \frac{1}{k}(\delta\phi_0 + n2\pi)$$

and

n - phase ambiguity index

k - wavenumber

\vec{B} - baseline vector

$\delta\phi_0$ - measured fractional phase difference

3. PROCEDURE

The recommended procedure for generating digital elevation surface models from the IFSAR data based on single-look complex images as output from the SAR image formation processor without resampling for geometric correction of the image distortions. Following generation of the two single-look complex images from each receive channel of the IFSAR, the data is first phase calibrated. This operation involves correcting for the

systematic phase difference inherent in the two receive chains. Typically the calibration signal is available as an auxiliary data channel from the radar sensor and recorded along with the backscatter data.

Following the phase calibration, the image derived from the Channel 1 (reference channel) data is multiplied by the complex conjugate of the Channel 2 image. In the resulting complex image, the Doppler, range and interferometric SAR phase difference information can be used to solve sequentially in closed form for the $\{x,y,z\}$ position of the target. The resulting target position is in the same coordinate system as the sensor position (e.g., WGS 84).

Each resolution cell in the complex image following the conjugate multiply operation can be converted to a three dimensional point in the output grid. The set of all such surface sample points provides an irregularly spaced collection of points which, in the absence of uncompensated systematic errors are statistically distributed and can be expected to lie on the true surface. Because the phase difference measurement is noisy, it is important to first smooth the phase difference values by multi-looking in the range/Doppler image plane. The averaged data can be used to compute the irregularly spaced terrain sample set.

The recommended approach to reduce the effects of noise in the surface sample points and to remove multiple values for surface elevations is shown in Figure 4. The multi-look averaging should include weights to account for variation in phase difference precision as a function of the received S/N, variation in cross range spacing as a function of range and other effects which indicate one sample is more precise than another.

The result of the smoothing process is an irregularly spaced (in planimetric position) set of weighted average points expected to lie on the actual surface. This set of points can be used to interpolate a regularly spaced DEM through standard surface interpolation techniques. For large images, the DEM computation (in fact, the entire process) can be subdivided into manageable slightly overlapping regions and the resulting pieces can be easily reassembled.

4. ERROR ANALYSIS

The accuracy of the derived DEM is limited by knowledge of the synthetic array state (i.e., position, velocity and attitude as a function of time over the synthetic aperture). For example, a radial position error results in a range pixel location, a range scale error and a cross-range location error. The technique is especially sensitive to errors in knowledge of the electronic boresight to the antenna. An error in the look angle, for

Complex Conjugate Multiply Image

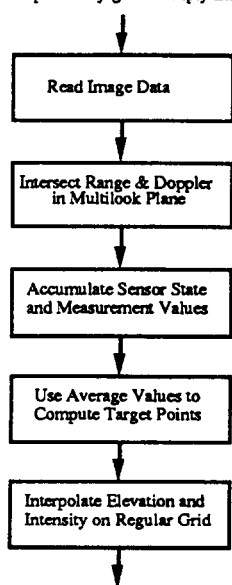


Figure 4. Flowchart for DEM and Ortho-Image Creation

example due to uncertainty in the platform roll angle, results in a cross-track scale error and a tilt in the derived DEM. In most cases if ground control is available, the errors resulting from poor attitude and ephemeris determination can be corrected such that the DEM is free from these systematic errors.

The sensor performance is also a predominant factor in the accuracy of the derived DEM. The phase noise in the complex image after the conjugate multiply operation, is typically the limiting factor in the accuracy of the derived DEM. This error source is random and can not be calibrated out of the DEM. Two dominant sources of phase noise are the thermal noise introduced primarily by the sensor electronics and the speckle noise resulting from a large number of independent scatterers per resolution cell.

The height estimation uncertainty resulting from random phase errors is given by (Li and Goldstein, (1989):

$$\sigma_h = \frac{\lambda R \sigma_\phi}{2\pi B \sin(\theta + \alpha)}$$

where σ_h is the standard deviation of the height estimation, σ_ϕ is the phase standard deviation, B is the baseline separation between antennas, λ is the radar wavelength, θ is the look angle, α is the roll angle and r is the sensor to target range distance.

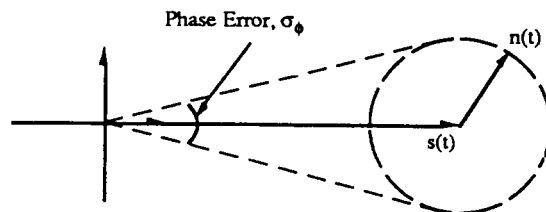


Figure 5. Illustration of the effect of thermal noise on the phase error estimate.

The above equation states that as the baseline separation between antennas is increased, the height estimation error is reduced for a given phase error. However as the baseline is increased the phase error associated with the speckle noise increases. The net effect is that there is an optimal separation between the antennas that is dependent on the signal to thermal noise ratio, the slant range and the slant range resolution (Prati, et al., 1990). A rule of thumb is that for a large signal to noise ratio (>20 dB) the optimal baseline is on the order of

$$B = \frac{0.2\lambda R}{\delta R_s}$$

where δR_s is the slant range resolution. Typically for a two antenna configuration on a single aircraft, the antennas are much closer together than the optimal separation and it is always advisable to space the antennas as far apart as possible.

6. REFERENCES

- Curlander, J. (1982). "Location of Spaceborne SAR Imagery", IEEE Geoscience and Rem Sens, GE-20, 359-364.
- Goldstein, R. H. Zebker and C. Werner (1988). "Satellite Radar Interferometry: Two-dimensional Phase Unwrapping", Radio Science, 23, 713-720.
- Li, F. and R. Goldstein (1989). "Studies of Multi-baseline Spaceborne Interferometric Synthetic Aperture Radars", IEEE Trans. Geoscience and Rem Sens, GE-28, 88-97.
- Prati, C., F. Rocca A. Monti Guarnieri and E. Damonti, 1990, Seismic migration for SAR Focusing: Interferometrical Applications, IEEE Trans. Geoscience and Remote Sensing, GE-28, 627-639.
- Zebker, H and R. Goldstein (1986). " Topographic Mapping from Interferometric Synthetic Aperture Radar Observations", J. Geophys. R., 91, 4993-4999.